



Isoprene emission and photosynthesis during heat waves and drought in black locust

Ines Bamberger¹, Nadine K. Ruehr¹, Michael Schmitt¹, Andreas Gast¹, Georg Wohlfahrt²,
Almut Arneth¹

5 ¹Institute of Meteorology and Climate Research - Atmospheric Environmental Research, Karlsruhe Institute of Technology (KIT/IMK-IFU), Garmisch-Partenkirchen, Germany

²Institute of Ecology, University of Innsbruck, Innsbruck, Austria

Correspondence to: Ines Bamberger (ines.bamberger@kit.edu)

Abstract. Extreme weather conditions, like heat waves and drought, can substantially affect tree physiology and the emissions of biogenic volatile organic compounds (BVOC), including isoprene. To date, however, there is only limited understanding of BVOC emission patterns during prolonged heat and coupled heat–drought stress as well as post-stress recovery. To assess the impacts of heat and heat–drought stress on BVOC emissions, we studied gas exchange and isoprene emissions of black locust trees under controlled environmental conditions. Leaf gas exchange of isoprene, CO₂ and H₂O was quantified using branch chambers connected to a proton-transfer-reaction mass spectrometer and an infrared gas analyzer. Heat and heat–drought stress resulted in a sharp decline of photosynthesis and stomatal conductance. Simultaneously, isoprene emissions increased six- to eight-fold in the heat and heat–drought treatment and resulted in a carbon loss that was equivalent to 12 % and 20 % of assimilated carbon at the time of measurement. Once temperature stress was released at the end of two 15 days long heat waves, stomatal conductance remained reduced, while isoprene emissions and photosynthesis recovered quickly to values of the control trees. Further, we found isoprene emissions to co-vary with net photosynthesis during non-stressful conditions, while during the heat waves, isoprene emissions could be solely described by non-linear functions of light and temperature. However, when isoprene emissions between treatments were compared under the same temperature and light conditions (e.g., T = 30°C, PAR = 500 μmol m⁻²s⁻¹), heat and heat–drought stressed trees would emit less isoprene than control trees. Our findings suggest that different parameterizations of light and temperature functions are needed in order to predict tree isoprene emissions under heat and combined heat–drought stress.

1 Introduction

Under a warming climate, extreme weather conditions, like heat waves and drought, are observed to occur more frequently (Coumou and Rahmstorf, 2012). Forested ecosystems contribute the majority of the global emissions of volatile organic compounds to the atmosphere (Guenther et al., 2012) and these emissions are expected to change with increasing frequency and intensity of climate extremes (Staudt and Peñuelas, 2010), which might persist following stress release. Up to now, however, there is only limited understanding of biogenic volatile organic compound (BVOC) emissions from trees during prolonged heat and combined heat–drought stress, including emission patterns during post-stress recovery.



With annual estimates ranging from 350 Tg yr⁻¹ to 800 Tg yr⁻¹, isoprene contributes most to the global budget BVOC emissions (Guenther et al., 2012). Influencing tropospheric ozone and methane levels (Atkinson, 2000) and the formation of secondary organic aerosols (Carlton et al., 2009), isoprene plays an important role in atmospheric chemistry and has an indirect effect on climate. Global isoprene emissions are most often estimated
40 using the so-called Guenther algorithms taking into account the temperature, and light dependency of emissions (Guenther et al., 1991, 1993, 2006). In these algorithms a species-specific standard emission factor (E_s , a constant which describes leaf emissions at standard conditions of typically 30°C and a photosynthetic active radiation of 1000 $\mu\text{mol m}^{-2} \text{s}^{-1}$) is multiplied with temperature and light functions. Guenther algorithms have been successfully used to model isoprene fluxes at spatial scales ranging from ecosystem to global level (e.g.
45 Brilli et al., 2016; Guenther et al., 2006, 2012; Lathière et al., 2006; Naik et al., 2004; Potosnak et al., 2013). However, the temperature and light functions depend on empirically derived parameters, which may not be constant across different regions, climatic conditions, or during weather extremes (Arneth et al., 2008; Niinemets et al., 2010b). Especially, the isoprene emission factor is well known to vary, even within a given species, for instance in response to weather extremes (Niinemets et al., 2010a). Thus the modeling algorithms often fail to
50 reproduce isoprenoid emissions of ecosystems under stress, irrespective of whether stress is induced mechanically or by drought (Kaser et al., 2013; Potosnak et al., 2013). Owing to the sparse amount of data, accounting for stress-induced BVOC emissions is one weak point of global BVOC models (Guenther, 2013; Niinemets et al., 2010a) and calls for further research in this area.

Unlike other volatiles, isoprene emissions by plants are constitutive and their emission pathway is relatively well known (Loreto and Schnitzler, 2010). Plants usually synthesize isoprene via the methylerithriol phosphate pathway (MEP) using carbon pools from photosynthesis (Sharkey and Yeh, 2001). Isoprene emission requires *de novo* synthesis, meaning that isoprene emissions from plants are predominantly dependent on enzymatic activity (Sharkey and Yeh, 2001). As a consequence, isoprene emissions are usually both, temperature, and light dependent (Niinemets et al., 2004). While under normal conditions only 1-2 % of the carbon fixed during
60 photosynthesis are emitted as isoprene (Harrison et al., 2013) this fraction may increase up to 50 % under stress (Loreto and Schnitzler, 2010; Pegoraro et al., 2004), resulting in the question why plants invest so much carbon to maintain isoprene production during periods of stress. Not all plants have the capacity to emit isoprene and its importance for plants is still not completely resolved (Harrison et al., 2013). However, it was suggested that isoprene helps to protect the photosynthetic apparatus during oxidative and thermal stress (Behnke et al., 2007;
65 Harrison et al., 2013; Siwko et al., 2007; Velikova and Loreto, 2005; Vickers et al., 2009) and therefore maybe an important mechanism in heat and drought tolerance

Episodic environmental stress conditions caused by heat waves or soil water deficit may increase significantly in frequency and/or severity under a future climate (Coumou and Rahmstorf, 2012). Drought periods are often combined with high temperatures (Boeck and Verbeeck, 2011). While some efforts have been made to quantify
70 isoprene emissions under stress conditions like high temperature stress (Sharkey and Loreto, 1993; Singsaas and Sharkey, 2000) or soil water deficit (Brilli et al., 2007, 2013; Funk et al., 2005; Loreto et al., 2006; Pegoraro et al., 2004), a complete and quantitative understanding of the effects of high temperatures on isoprene emissions, especially if they occur in combination with drought has not yet been reached.



75 Broadleaf deciduous tree species cover about one-third of the global land area, but are estimated to be responsible for the majority of global BVOC emissions (Guenther, 2013). Black locust (*Robinia pseudoacacia* L.), a broadleaf tree and relatively strong isoprene emitter (Kesselmeier and Staudt, 1999), originally native in North America is nowadays quite commonly planted also in Europe (Cierjacks et al., 2013). Due to its rapid growth and its comparatively high tolerance to stress (e.g. drought stress, Mantovani et al., 2014) the area of where the tree species is grown is expected to further increase under a warmer climate (Kleinbauer et al., 2010).

80 The objectives of this study were therefore, (1) to quantify the effect of heat and combined heat–drought stress on isoprene emissions of black locust trees as well as the successive emission recovery, (2) to gain more insights in the fraction of recently assimilated photosynthetic carbon used for isoprene emission especially under stressful conditions, and (3) to evaluate empirical temperature and light response curves of isoprene emissions under abiotic stress. A greenhouse experiment with two week-long heat waves (+10°C above control trees) was

85 conducted, followed by a recovery period of one week at ambient temperatures. During the experiment, isoprene emissions of black locust trees were measured concurrently with the CO₂ and H₂O gas exchange using an automated leaf chamber setup.

90



2 Materials and methods

2.1 Experimental set-up

Black locust seedlings (*Robinia pseudoacacia* L.) were grown in a greenhouse facility in Garmisch-Partenkirchen, Germany (708 m a.s.l.). The trees had been planted in individual large pots (120 l) filled with a mixture of humus and sand (ratio of 2:3) in September 2012. In 2014, when the experiment was conducted, trees were four-years old. Trees in the stress treatments had already been exposed to two experimental heat waves during summer 2013, the basal area of the previously heat exposed trees was larger by 36 % compared to previously heat-drought exposed trees (Ruehr et al., 2016). After the experiment in 2013 ended, the trees were pruned to 1.80 m height, kept outside during winter, and relocated into the greenhouse in May 2014, where the measurements were performed from 10th of July until 26th of August.

During the experimental phase, trees were kept in two neighboring, but separately controllable compartments of the greenhouse. Differences in environmental conditions between the two compartments of the greenhouse were generally small during both years of the experiment (Ruehr et al. 2016, Duarte et al., 2016). While in one compartment of the greenhouse, trees were always kept under ambient conditions (control trees), trees in the second compartment (heat and heat-drought trees) were periodically exposed to two consecutive heat waves simulated by a 10°C increase of temperature lasting 14-15 days. During the heat waves, relative humidity in the heat compartment of the greenhouse was decreased so that vapor pressure deficit increased considerably. Each heat wave was followed by a recovery phase of 7 days. While control and heat-treated trees received on average 2.6 l tree⁻¹ day⁻¹ irrigation, heat-drought treated trees received (starting 6 days before heat stress) only 1.3 l tree⁻¹ day⁻¹. Recovery periods were initiated by supplying each tree once with a larger amount of water (10.8 l) which should have increased soil moisture by roughly 10 % and thus largely reduce soil water deficit. Isoprene emissions were measured in parallel to CO₂ and H₂O gas exchange using leaf chambers attached to three different trees per treatment. Leaf biomass and the specific leaf area were used to determine the half sided leaf area within the leaf chambers. In case a leaf attached to one of the leaf chambers dried out during the heat waves (which happened once during the first heat wave in the heat-drought treatment) the leaf was replaced inserting an intact leaf of the same tree into the corresponding chamber. To determine litter fall in the in the heat and heat-drought treatment, dried or yellow leaves were collected during the stress periods and the dry weight of the leaf litter was measured and leaf area calculated.

The environmental conditions in the greenhouse (equipped with UV-transmissive glass) were regulated by a computer (CC600, RAM Regel- und Messtechnische Apparate GmbH, Herrsching, Germany). The bottom of each tree pot was equipped with a coiled water pipe to provide soil cooling to mimic pre-defined soil temperatures at a depth of 50 cm (corresponding to air temperature averaged over previous 20 days). Soil water content (10HS, Decagon Devices, Inc, Pullman, WA, USA) and soil temperature (T107, Campbell Scientific Inc., UT, USA) were measured in each pot at a depth of 10 cm and in additional pots at 30 and 50 cm depth. The volumetric soil water content (SWC) was used to determine the daily relative extractable soil water (RSW, in %) according to following relationship

$$RSW = 100 \times \frac{SWC - SWC_{\min}}{SWC_{\max} - SWC_{\min}}, \quad (1)$$



with, SWC_{min} and SWC_{max} being experimentally derived minimum values of daily soil water content at 30 cm depth during drought and maximum values of mean daily SWC per sensor. In order to get an average value per tree pot, RSW from three different depths were averaged.

2.1.1 Automated leaf chamber set-up

The gas exchange of black locust leaves was measured using a self-made, automated chamber system on three trees per treatment, and one empty chamber. The chambers were constructed from transparent cylinder, enclosed by two caps (inner volume: 6.65 l) all made of acrylic glass (PMMA, Sahlberg, Feldkirchen, Germany) coated with a FEP (fluorinated ethylene propylene, PTFE Spezialvertrieb, Stuhr, Germany) foil to ensure chemical inertness of the interior of the chamber. For easy insertion of the leaf petiole during installation, the cap on the tree-facing side could be taken apart. The other cap was opened and closed automatically using pressurized air (6 bar). We minimized gas leakage by sealing with PTFE foam, transparent tape and plastic sealing band (Teroson, Düsseldorf, Germany) between branch, lids and chamber body. During chamber measurements, a 12 V fan (412 FM, EBM-Papst, Mulfingen, Germany) was constantly running to provide homogeneous mixing inside the plant chamber.

To produce CO_2 , water vapor and VOC and O_3 free zero air, outside air was drawn by an oil free scroll compressor (SLP-07E-S73, Anest Iwata, Japan) through an Ultra Zero Air Generator (N-GT 30000, LNI Schmidlin SA, Geneve, Suisse). In parallel, a second air stream (Liquid Calibration Unit, Ionicon, Innsbruck, Austria) added CO_2 and H_2O to the zero air at a rate of 1 nL min^{-1} (normalized liter per minute). Together a constant flow of 7 sl min^{-1} , containing $409 \pm 11 \mu\text{mol mol}^{-1} CO_2$, $6.1 \pm 0.4 \text{ mmol mol}^{-1} H_2O$, and VOC free air, was routed to the chambers (Fig. 1).

The main tubing line of the chamber set-up was 3/8 inch stainless steel tubing (Swagelok, Ohio, USA) coated with SilcoNert (Silco Tek GmbH, Bad Homburg, Germany). The direction of air flow to the different chambers was controlled by 2/ solenoid valves with PTFE housing (0121-A-6,0-FFKM-TE, Bürkert, Ingelfingen, Germany) connected by a 3/8 inch PTFE tube (ScanTube GmbH, Limburg, Germany) to the inlet and outlet of the leaf chambers (Fig. 1). Another valve placed in the center of the main tubing (see Fig. 1 V_{main}) could be opened to flush the entire system with VOC-free air.

During the automatic switching between the individual leaf chambers and the empty chamber (performed by controlling valves and fans via ICP modules, I-7067D, ICP DAS, Hsinchu County, Taiwan), each chamber was sampled for at least eight minutes. Between the measurements of different chambers the tubing was flushed with the VOC-free synthetic air for one minute.

In each chamber, air temperature was measured by a thermocouple (5SC-TT-TI-36-2M, Newport Electronics GmbH, Deckenpfronn, Germany) and light conditions by a photodiode optimized to measure photosynthetic active radiation (G1118, Hamamatsu Photonics, Hamamatsu, Japan). Photodiodes were cross-calibrated using a photosynthetic active radiation (PAR) sensor (PQS 1, Kipp & Zonen, Delft, The Netherlands).



165 **2.1.2 Water vapor and carbon dioxide exchange**

Concentrations of CO₂ and H₂O in the ingoing and outgoing airstream were measured by a Li-840 (for absolute concentrations) connected to a Li-7000 (LI-COR Inc., Lincoln, NE, USA) running in differential mode (Fig. 1). This allowed measuring differences between ingoing and outgoing air concentrations, as well as absolute concentrations. The three measurement cells of both infrared gas analyzers (IRGA) were supplied with 0.5 l min⁻¹ each, provided by a pump (NMP830KNDC, KNF, Freiburg, Germany), connected to a mass flow controller (F-201CV-1K0-RAD-22-V, Bronkhorst, Ruurlo, NL). The two measurement cells of the Li-7000 were matched regularly and recalibrated with the Li-840 on a bi-weekly basis. To detect and remove any offsets not influenced by plant gas exchange between outgoing and ingoing air, measurements of an empty chamber were performed. To calculate gas exchange rates, we determined average concentration differences (air_{delta}= air_{out}- air_{in}) under steady state conditions (between 300s and 490 s after chamber closure). Steady state criteria were reached when the standard deviation of averaged differences (within the above defined time frame for steady state) in water vapor (ΔH_2O) was < 0.5 mmol mol⁻¹ and the rate of change in ΔH_2O over time was < 0.01 mmol s⁻¹. Transpiration (Tr in mmol m⁻² s⁻¹) was calculated using the following equation

$$Tr = \frac{f \Delta H_2O}{l_a \left(1 - \frac{H_2O_{out}}{1000}\right)}, \quad (2)$$

180 where f is the air flow rate in mol s⁻¹, ΔH_2O the difference in water vapor between ingoing and outgoing air (H₂O_{out}) in mmol mol⁻¹, and l_a the half-sided leaf area in m².

Photosynthesis (A in $\mu\text{mol m}^{-2} \text{s}^{-1}$) was assumed to reach steady state when the standard deviation of the averaged differences (within the above defined time frame for steady state) in CO₂ between ingoing and outgoing air (ΔCO_2) was < 2.5 $\mu\text{mol mol}^{-1}$ and the rate of change in ΔCO_2 was < 0.2 $\mu\text{mol mol}^{-1}$, and was then derived as follows

$$A = \frac{f \Delta CO_2}{l_a} - \frac{(CO_{2\ out} Tr)}{1000}, \quad (3)$$

where $CO_{2\ out}$ is the CO₂ concentration of the outgoing air in $\mu\text{mol mol}^{-1}$ corrected for dilution by transpiration. Stomatal conductance (g_s in mol m⁻² s⁻¹) was calculated from transpiration using the following formula

$$g_s = \frac{Tr (1000 - \frac{W_L \Delta H_2O}{2})}{W_L - \Delta H_2O}, \quad (4)$$

190 with, W_L referring to the molar concentration of water vapor in the leaf (in mmol mol⁻¹) as calculated from the ratio of the saturation vapor pressure at a given leaf temperature and the atmospheric pressure (both given in kPa).



195 **2.1.3 Volatile organic compounds**

Measurements of isoprene emissions were performed using a high sensitivity proton-transfer-reaction mass spectrometer (PTR-MS, IONICON, Innsbruck, Austria) operated at a drift tube pressure of 2.3 mbar, and a temperature and voltage of 60°C and 600 V along the drift tube, respectively. The operation principle of the PTR-MS is described elsewhere (Hansel et al., 1995; Lindner et al., 1998). The PTR-MS was operated to sequentially measure a set of preselected mass channels (assignable to BVOCs) including isoprene (m/z 69).

At regular intervals, calibrations of the PTR-MS at ambient humidity were conducted routing an air mixture containing several volatile organic compounds at predefined mole fractions of 7 ppb, 10 ppb, 15 ppb and 20 ppb through the instrument (Fig. 1). The air mixture was provided by a liquid calibration unit diluting a gas standard (IONICON, Innsbruck, Austria) containing 15 different volatile organic compounds in N₂ at ppm levels with 205 VOC-free zero air. During the measurements in 2014, the sensitivity for isoprene was determined to be between 7.0 and 7.3 ncps ppb⁻¹ (normalized counts per second and ppb, normalized to a drift tube pressure of 2.2 mbar and 1 million primary ions). The limit of detection for isoprene was determined to be around 0.4 ppb at an integration time of one second.

The isoprene flux (E_{iso} in nmol m⁻²s⁻¹) was calculated according to Niinemets et al. (2011)

210
$$E_{iso} = (c_{out,c} - c_0) \frac{f}{t_a} \quad (5)$$

Where $c_{out,c}$ is the VOC concentration (in nmol mol⁻¹) measured at the outlet of the branch chamber, c_0 is the VOC concentration measured at the output of an empty chamber. With the subtraction of the VOC concentration measured at the outlet of an empty chamber (c_0), fluxes were corrected for the VOC background in the zero air and possible fluxes from/to the empty chamber and the associated tubing. The empty chamber background for 215 isoprene contributed on average only two percent to the total isoprene signal measured in the control plant chambers. Since the transpiration correction (rightmost term of Eq. (3)) for the control, heat and heat-drought chambers contributed on average less than 0.5 % of the daytime (PAR > 50 μmol m⁻²s⁻¹) isoprene emissions, it was neglected. Isoprene concentrations reached their equilibrium usually about one minute later than CO₂ and H₂O concentrations and VOC measurements showed a larger level of noise compared to CO₂ and H₂O 220 concentrations, so the quality criteria for isoprene differed from the criteria for CO₂ and H₂O exchange. To avoid systematic errors due to an insufficient air exchange in the chambers only isoprene concentrations during the last minutes of each chamber closure (after 360 s of closure until the end) were averaged to calculate the equilibrium isoprene fluxes (Eq. (5)). Measurements (a) when chambers were not closed sufficiently long (less than 420 s), (b) when the performance of the PTR-MS was inadequate (e.g. directly after refilling the water bottle), or (c) 225 when no empty chamber measurements were available, were discarded.

2.2. Modeling the temperature and light responses of isoprene

Since isoprene emissions from plants are temperature and light dependent, leaf level isoprene fluxes can be estimated from a light-dependent function f_Q , a temperature dependent function f_T , and an isoprene emission



230 factor E_S which is assumed to be a constant, but plant-specific factor which describes the isoprene emissions at reference conditions (e.g., a temperature of 30°C and PAR=500 $\mu\text{mol m}^{-2}\text{s}^{-1}$).

$$E_{iso} = E_S f_Q f_T \quad (6)$$

235 Temperature and light response functions are usually normalized to unity at standardized conditions and describe the shape of the isoprene emission curve. The response functions were first developed by Guenther et al. (1991, 1993). These models use a hyperbolic function to describe the light response function as follows

$$f_Q = \frac{C_{L1}\alpha Q}{\sqrt{1+\alpha^2 Q^2}}, \quad (7)$$

240 where C_{L1} is a scaling constant and α the quantum yield of isoprene emission; here, both parameters were optimized for each treatment separately in order to best describe the light response function of the measured isoprene fluxes.

The temperature dependency of isoprene emissions is usually characterized by an exponential increase with leaf temperature until an optimum temperature T_{opt} is reached followed by a subsequent exponential decrease (Guenther et al., 1991, 1993).

$$f_T = \frac{e^{\left(\frac{C_{T1}(T_L-T_S)}{RT_S T_L}\right)}}{1+e^{\left(\frac{C_{T2}(T_L-T_{opt})}{RT_S T_L}\right)}} \quad (8)$$

245 T_s is a standard temperature (usually 30°C) at which the normalized response curve is one, R is the gas constant (8.314 $\text{J mol}^{-1} \text{K}^{-1}$), T_L is the leaf temperature in Kelvin and C_{T1} and C_{T2} are parameters which can be interpreted as activation and deactivation energy of isoprene emissions (in J mol^{-1}), respectively. The experimentally derived average temperature response of the control, heat and heat-drought treated trees was used to optimize the parameters C_{T1} , C_{T2} and T_L using a nonlinear weighted fitting algorithm (see Section 2.4) for each treatment 250 separately. For the control treatment we did not have enough data points in the high temperature range to constrain the optimum temperature, and therefore set the optimum temperature to a fixed value of 311.8 K (see Guenther et al., 1991) in order to optimize the remaining parameters.

2.3 Data analysis and statistics

255 The data post-processing and statistical calculations were performed using the commercial software package Matlab® (Version R2013b, Math Works®, MA, USA). To estimate leaf isoprene emissions we largely followed the standardization criteria (except for light control) for leaf-scale emission measurements recommended by Niinemets et al. (2011). Because temperature control was performed within the separate compartments of the greenhouse temperatures within the leaf chambers were recorded, but not controlled separately.



260 Increases or decreases in isoprene emissions and photosynthesis during the heat waves were calculated as treatment effect ($\frac{\text{treatment-control}}{\text{control}}$). To test for differences between treatments and time periods, we used a linear mixed effects model (using fixed effects for time period and treatment and random effects for tree and measurement day) to test for significant changes in daily average isoprene emissions for each treatment and during the different time periods of the experiment (Ruehr et al., 2016).

265 To determine light and temperature relationships of isoprene emissions in each treatment and during both stress periods, we grouped the data into 8 bins according to PAR levels ($<5 \mu\text{mol m}^{-2}\text{s}^{-1}$, $5\text{--}50 \mu\text{mol m}^{-2}\text{s}^{-1}$, $50\text{--}100 \mu\text{mol m}^{-2}\text{s}^{-1}$, $100\text{--}150 \mu\text{mol m}^{-2}\text{s}^{-1}$, $150\text{--}200 \mu\text{mol m}^{-2}\text{s}^{-1}$, $200\text{--}400 \mu\text{mol m}^{-2}\text{s}^{-1}$, $400\text{--}650 \mu\text{mol m}^{-2}\text{s}^{-1}$ and $> 650 \mu\text{mol m}^{-2}\text{s}^{-1}$) and temperature conditions ($15\text{--}20^\circ\text{C}$, $20\text{--}24^\circ\text{C}$, $24\text{--}28^\circ\text{C}$, $28\text{--}32^\circ\text{C}$, $32\text{--}35^\circ\text{C}$, $35\text{--}40^\circ\text{C}$, $40\text{--}45^\circ\text{C}$ and $>45^\circ$) within the chambers. The parameterization of the light and temperature response functions (Eq. (7) and (8)) was done for each treatment as follows. In an initial step, the bin-averaged isoprene data (PAR $> 50 \mu\text{mol m}^{-2}\text{s}^{-1}$ with temperature bins defined above) were fitted to the temperature-response function (Eq. 8) using a non-linear fitting algorithm weighted with the inverse standard deviation. The gained temperature fit (parameter EF, CT₁, CT₂ and T_m) was then used to normalize the measured isoprene emissions to a standard temperature of 30°C before fitting isoprene data bin-avaraged for PAR to the light-response function (Eq. 7). The gained light-response fit (parameter E_{light} and α) was then used to normalize the measured isoprene flux data to standard light levels (PAR = $500 \mu\text{mol m}^{-2}\text{s}^{-1}$), which were then again fitted to the temperature-response function. This procedure was repeated in an iterative way until all fitting parameters changed by less than 1 % between subsequent iterations.

270

275

280 The fraction of recently assimilated carbon emitted as isoprene was calculated by dividing the isoprene carbon flux (5 C-atoms) by the assimilated carbon (1 C-atom) and calculating bin averages after classifying the isoprene fluxes for PAR $> 50 \mu\text{mol m}^{-2}\text{s}^{-1}$ into 8 temperature bins as mentioned above.



3 Results

285 3.1 Environmental conditions

With a maximum of 34.7°C and a minimum of 27.8°C, daily average air temperatures during the heat waves were considerably warmer than under ambient conditions (maximum 23.2°C and minimum 13.7°C). Along with warmer temperatures vapor pressure deficit (VPD) increased up to 3.0 kPa while under ambient conditions VPD remained below 1.0 kPa (Fig. 2b). Outside the stress periods air temperature and VPD did not differ between the 290 greenhouse compartments (Fig. 2a,b).

While the daily-averaged relative extractable soil water content (RSW) remained above 40 % in the control trees it decreased to 20 % in the heat and 15 % in the heat-drought treatment (Fig. 2c). After watering at the first day of the recovery, the soil water content in the stress treatments increased considerably and RSW during the recovery remained between 50 % and 70 % in all trees. During the heat periods, RSW of heat-stressed trees was 295 slightly higher than RSW of heat-drought stressed trees. Heat and heat-drought stress caused a large decline in midday leaf water potential (-1.7 MPa in the control compared to -2.3 MPa in both treatments, data not shown). In both treatments we observed pronounced leaf shedding during the first heat wave in 2014. We estimated that about 80 % of the leaves were shed in the heat treatment and 90 % in the heat-drought treatment, averaging in both treatments to a leaf area of about $2.4 \text{ m}^2 \text{ m}^{-2}$ lost. The relative larger leaf shedding and lower basal area (as a 300 result of the previous experiment) in the heat-drought trees likely were the cause for the relatively small treatment differences in RSW, despite irrigation in the heat-drought treatment being 50 % lower compared to the heat and control treatment. Generally, leaf shedding protects black locust from pronounced tree water deficits by reducing water loss via transpiration (Ruehr et al. 2016).

305 3.2 Stomatal conductance, photosynthesis and isoprene emissions

Along with increased temperatures and reduced relative extractable soil water content during the stress, daily-averaged stomatal conductance (PAR $> 50 \text{ } \mu\text{mol m}^{-2} \text{ s}^{-1}$) in heat-drought stressed trees decreased to values below $0.01 \text{ mol m}^{-2} \text{ s}^{-1}$ (Fig. 3a). The stomatal conductance of heat-stressed trees during the heat waves was, compared to heat-drought stressed trees, higher with daily averages between 0.01 and $0.03 \text{ mol m}^{-2} \text{ s}^{-1}$, but still 310 lower than in the control trees (Fig. 3a). Compared to the control, photosynthesis during the first heat wave decreased on average by 44 % in the heat and 67 % in the heat-drought treatment (Fig. 3b). During the second heat wave, photosynthesis decreased less compared to the control (by 41 % in the heat and by 46 % in the heat-drought treatment). A linear mixed effects model comparing photosynthesis during the stress periods in the heat and heat-drought treatment to pre-stress control conditions confirmed the significance of these changes 315 (Table 1).

Daytime (PAR $> 50 \text{ } \mu\text{mol m}^{-2} \text{ s}^{-1}$) isoprene emissions of black locust in the heat treatment were on average by 153 % and 142 % higher than in the control trees during the first and second heat wave, respectively (Fig. 3c). For heat-drought stressed trees isoprene emissions were by 171 % higher than for control trees in the first heat wave and by 333 % in the second heat wave. During both recovery periods the isoprene fluxes decreased rapidly 320 to values comparable to pre-stress conditions, suggesting a quick and complete recovery. The significance of



changes in isoprene emissions in the heat and heat-drought treatment during stress and recovery was confirmed by a linear mixed effects model. The model showed a significant ($p\text{-value} < 0.05$) or at least marginally significant ($p\text{-value} \text{ around } 0.1$) treatment effect during the heat waves, while before stress and during the two recovery phases isoprene emissions did not differ significantly ~~between~~ treatments (Table 1). Irrespective of treatment and time period, nighttime fluxes of isoprene were always zero.

325

3.3 Relationship between CO₂ and isoprene emissions under stress conditions

We found isoprene emissions of the heat and heat-drought treated trees during the recovery periods to be clearly related to photosynthesis (A) following an exponential function $E_{\text{iso}} = \exp(a^*A) - b$ ($p\text{-value} < 0.05$; Fig. 4). Such a relationship was also visible in control trees as long as temperatures did not exceed 30°C (Fig. 4). In control trees net photosynthesis was on average 4.5 $\mu\text{mol m}^{-2}\text{s}^{-1}$ and isoprene emission 1.5 $\text{nmol m}^{-2}\text{s}^{-1}$ on average. During the heat waves, isoprene emissions ~~were~~ not related to photosynthesis anymore in heat and heat-drought treated trees. Net photosynthesis decreased to 2.5 $\mu\text{mol m}^{-2}\text{s}^{-1}$ on average in the heat and 2.1 $\mu\text{mol m}^{-2}\text{s}^{-1}$ on average in the heat-drought treatment, while isoprene fluxes increased sharply to 11.2 $\text{nmol m}^{-2}\text{s}^{-1}$ on average in the heat and 5.9 $\text{nmol m}^{-2}\text{s}^{-1}$ on average in the heat-drought treatment.

335



In the temperature range from 28°C to 32°C, control trees emitted carbon equivalent to 1.6 % of assimilated carbon as isoprene (Table 2). In the same temperature range, heat and heat-drought stressed trees emitted carbon equivalent to 0.8 % (significantly different to control trees) and 1.2 % (no significant difference compared to control) of the photosynthetic carbon as isoprene, respectively. With increasing temperatures, heat-stressed trees emitted what would be up to 12 % (temperature $> 45^\circ\text{C}$) of the assimilated carbon as isoprene and heat-drought stressed trees up to 20 % (40 $<$ temperature $<$ 45°C).

340

3.4 Changes in light and temperature curves of isoprene during stress

The ~~stress responses of~~ light and temperature relationships of isoprene were assessed for all treatments during the heat waves only (Table 3). Details for all parameters optimized by recursively fitting the nonlinear light and temperature equations (Eq. (7) and (8)) to the bin-averaged isoprene curves are given in Table 3. Except for the parameter C_{T1} in the heat-drought treatment all fitted values were statistically significant ($p\text{-value} \leq 0.05$).

345

Control trees emitted, normalized to a photosynthetic active radiation of 5 $\text{nmol m}^{-2}\text{s}^{-1}$, constantly more isoprene than stressed trees at similar temperatures (Fig. 5b). The 95 % confidence bounds for the fitted curves (dashed lines) indicate that temperature functions of heat and heat-drought trees were statistically different to the temperature function of control trees. At a standard temperature of 30°C, for example, control trees emitted $16.0 \pm 0.2 \text{ nmol m}^{-2}\text{s}^{-1}$ of isoprene, while heat-stressed trees and heat-drought stressed trees emitted $8.7 \pm 0.5 \text{ nmol m}^{-2}\text{s}^{-1}$ and $12.1 \pm 1.2 \text{ nmol m}^{-2}\text{s}^{-1}$, respectively (see also Table 2). Similarly, the relationship of photosynthetic active radiation with isoprene emissions (Fig. 5a, normalized to a temperature of 30°C) showed that at light saturation, control trees ($16.2 \pm 1.4 \text{ nmol m}^{-2}\text{s}^{-1}$) emitted considerably more isoprene than heat, and heat-drought stressed trees (9.5 ± 0.4 and $12.8 \pm 0.7 \text{ nmol m}^{-2}\text{s}^{-1}$, respectively). Compared to literature values

350

355



isoprene emissions of all trees reached light saturation at relatively low values of photosynthetic active radiation (e.g. PAR between 200 and 300 $\mu\text{mol m}^{-2}\text{s}^{-1}$ for the control and heat-drought stressed trees) most probably because they were adapted to comparatively low levels of PAR in the greenhouse and only the leaves in the
360 lower part of the canopy were measured.



4 Discussion

4.1 Stress response and recovery

365 In our study, heat and heat-drought stressed trees showed reduced stomatal conductance along with lower rates of carbon assimilation during the heat waves (Fig. 3). While photosynthesis in black locust is limited by stomatal closure during heat and heat-drought stress (Ruehr et al., 2016), isoprene emission is mostly insensitive to the degree of stomatal opening (i.e., high Henry's law constant see Niinemets et al., 2004). Additionally the temperature optimum of photosynthesis is usually exceeded at much lower temperatures than that for isoprene synthase activity (Rennenberg et al., 2006) resulting in an earlier inhibition of photosynthesis compared to isoprene emissions (Loreto and Fineschi, 2015). In this experiment, heat and heat-drought stressed black locust trees showed a temperature optimum of photosynthesis at about 25°C, while peaks in isoprene emissions were reached at much higher temperatures (42.4°C in the heat and 41.2°C in the heat-drought treatment) similar to what has been reported for other tree species (Guenther et al., 1991, 1993; Monson et al., 1992). The temperature optima of isoprene synthase and other enzymes are likely responsible for this threshold (Ninemets et al., 2010a) and we can expect isoprene emissions to increase unless these temperature optima are reached or carbon substrate for isoprene synthase has become depleted (Grote and Niinemets, 2008). In agreement, early studies on heat stress responses found elevated isoprene emissions (Sharkey and Loreto, 1993; Singsaas and Sharkey, 2000). This is in stark contrast to patterns of isoprene emissions during drought, where most studies found no change or even reduced emissions (Brilli et al., 2007; Fortunati et al., 2008). In our study, however, the effects of drought were apparently dominated by the responses of isoprene emissions to the high temperatures as both heat and heat-drought stress trees showed similar emissions. This may indicate that hotter droughts as predicted with climate change could lead to enhanced isoprene emissions in black locust.

385 Upon stress release, isoprene emissions recovered more quickly (within about two days) than photosynthesis to pre-stress levels. A quick recovery of isoprene emissions after periods of drought stress seems to emerge as a common feature that has also been observed in previous studies (Li et al., 2013; Pegoraro et al., 2004; Velikova and Loreto, 2005) and may help isoprene emitting plants to cope with abrupt and repeated temperature changes as commonly observed under natural conditions. The observed faster recovery of isoprene emissions than photosynthesis may be a common pattern following stress release (Brilli et al., 2013; Pegoraro et al., 2004).
390 However, studies on isoprene dynamics following stress release are scarce and to our knowledge this is the first study that considers dynamics of isoprene emissions during and following combined heat-drought stress. In summary, fast recovery of both isoprene emission and photosynthesis suggests that no irreversible damage to the unshed leaf tissues in consequence of high temperature or drought (Ninemets, 2010) occurred.

395 **4.2 Isoprene emissions and photosynthetic carbon**

Photosynthesis supplies most of the carbon as well as energy for isoprene synthase during unstressed conditions (Karl et al., 2002; Niinemets et al., 1999; Sharkey and Loreto, 1993). Assuming that all the carbon incorporated into isoprene originates directly from photosynthesis, approximately 1.6 % of the assimilated carbon was used for isoprene emission in control trees at temperatures between 28°C and 32°C. This value is in the same range as



400 the 2 % which were proposed for other major isoprene emitting trees at a temperature of 30°C (Sharkey and Yeh, 2001; Sharkey et al., 2008). The ratio of photosynthesis to isoprene emission can however change dramatically during stress conditions. In a coppice poplar plantation at ambient temperatures only 0.7 % of assimilated carbon was emitted as isoprene (Brilli et al., 2016), while in response to high temperature or drought stress, the ratio of isoprene emission to assimilated C may increase up to about 50 % (Barro et al., 2004; Siwko et al., 2007). In our experiment we found the equivalent of up to 13 % of C assimilated in the heat and 20 % in the heat-drought treatment to be emitted as isoprene (Table 2). Although, the difference between the treatments is not significant the larger ratio of isoprene emission to photosynthesis could result from the lower photosynthetic rates in the heat-drought trees. While we assume that isoprene is mainly formed from current photosynthates, we cannot exclude that C for isoprene formation might have originated from other carbon sources such as sugars and starches. Especially under conditions of limited photosynthesis, like severe drought, it has been reported that plants use increasing amounts of stored carbon to supply the carbon need for isoprene synthesis (Brilli et al., 2007; Fortunati et al., 2008). The divergence between photosynthesis and isoprene emissions during stress as found in our study could indicate that re-mobilized carbon might have been used to supply isoprene synthesis, which could originate from non-structural carbohydrates in leaves or other tissues (Schnitzler et al., 2004).

415 It is still a matter of debate why some plants invest substantial amounts of carbon to maintain isoprene emissions even under severe stress when carbon demand for maintenance might be higher than carbon supply. One likely explanation is that isoprene acts as antioxidant in the plants eliminating reactive oxygen species produced during stress in order to prevent oxidative damage (Vickers et al., 2009). Further, isoprene is discussed to protect the chloroplasts under high temperatures or drought (Velikova et al., 2011; Velikova et al., 2016) which was explained with a stabilizing effect of isoprene on the thylakoid membranes (Velikova et al., 2011). This in turn has been again reported to reduce the formation of reactive oxygen species (Velikova et al., 2012). However, Harvey et al. (2015) found that the concentration of isoprene within the leaves is lower than expected and thus unlikely to alter the physical properties of the thylakoid membranes. Although the detailed pathways of isoprene emissions are still not completely elucidated (Monson et al., 2012), it is known, that isoprene emitting plants are able to cope better (meaning that they showed increased photosynthesis and electron transport rates) with high temperature episodes compared to their non-isoprene emitting competitors (Behnke et al., 2007). In the same way, isoprene emitting plants are known to recover more quickly after stress than plants which were isoprene inhibited (Velikova and Loreto, 2005). The results of our study agree with this theory, as photosynthesis in previously heat and heat-drought stressed black locust recovered fast although stomatal conductance remained reduced.

420

425

430

4.3 Changes of isoprene temperature and light response functions during stress

Common knowledge about the temperature response function of isoprene (Niinemets et al., 2010) would suggest that the higher isoprene emissions for stressed plants found here are solely due to increased temperatures. However, heat and heat-drought stressed trees showed somewhat different temperature and light response curves and had 45 % and 25 % lower isoprene emissions relative to the control trees at standard temperature (20°C). If isoprene emissions of the stress trees are calculated with the parameter values of control trees, the average isoprene emissions during stress would have been overestimated by 50 % in heat and by 68 % in heat-drought



440 trees. At a first glance the apparent lower isoprene emissions in stressed trees compared to unstressed trees at the same temperature is surprising because of the thermoprotective role of isoprene (Velikova and Loreto, 2005; Vickers et al., 2009). Intuitively one would expect heat and heat-drought stressed plants to emit – in comparison to control trees at the same temperature – more isoprene during periods of stress. However, the quantity of emissions might not be so important for the thermoprotective effect as long as isoprene emissions are maintained. Vickers et al. (2009) stated that even low isoprene emissions should be sufficient for the 445 stabilization of membranes under heat stress. A fact which supports this theory is that external isoprene fumigation of emitting plant species does not increase their thermotolerance (Logan and Monson, 1999), while isoprene fumigation of isoprene-inhibited plants is known to increase plant thermotolerance (Velikova and Loreto, 2005).

450 The overestimation of isoprene emissions simulated by the Guenther et al. algorithm during prolonged stress episodes agrees with observations at the ecosystem scale: Potosnak et al. (2013) found that isoprene emissions from an oak and hickory dominated deciduous forest were at the onset of a drought underestimated and with increasing severity of the drought overestimated by the Guenther et al. algorithm and Brilli et al. (2016) reported that during a high temperature period at a poplar plantation isoprene emissions simulated with the Guenther et al. 455 algorithm were higher than observed emissions. The reduction of isoprene emissions during stress period could be related to a change in the emission factor, while our study indicates that not only the emission factor but the shape of the temperature and light response functions were affected by prolonged heat and heat-drought stress. A reduction of isoprene emission rates under prolonged but moderate stress does not only hold for drought stress, but has been found for several abiotic stressors (Niinemets, 2010). It is also known that the severity and duration of stress plays a crucial role in the actual stress response especially in case of irreversible damage 460 (Niinemets, 2010).

465 It seems necessary to incorporate separate stress response functions into current BVOC emission models in order to estimate isoprene emissions under stress correctly. Most probably such stress response functions will need to be developed for different BVOC classes separately. For most BVOCs there exists, if at all, only a qualitative understanding of their response to prolonged abiotic stress. Therefore more studies are needed to quantify the effect of multiple stressors, e.g. heat combined with drought, and the effect of prolonged stress on BVOC emissions. Especially with regard to the increasing probability of weather extremes under a future climate an improved stress response in BVOC models would be vital for air quality models and future climate projections.

470 **Acknowledgements** We would like to thank the IMK-IFU IT and mechatronics team, especially Christoph Soergel, Stefan Schmid and Bernhard Thom for their support and Martina Bauerfeind for her lab assistance. Further we would like to acknowledge Jukka Pumpanen from the University of Eastern Finland, Kuopio for his advice with the chamber design and setup.

475 This research was supported by the German Federal Ministry of Education and Research (BMBF), through the Helmholtz Association and its research program (ATMO), and a grant to Almut Arneth from the Helmholtz Association Innovation and Networking fund. I. B. and N.K.R. acknowledge support by the German Research Foundation through its Emmy Noether Program (RU 1657/2-1).



References

480 Arnett, A., Monson, R. K., Schruggers, G., Niinemets, Ü. and Palmer, P. I.: Why are estimates of global terrestrial isoprene emissions so similar (and why is this not so for monoterpenes)?, *Atmos. Chem. Phys.*, 8(16), 4605–4620, doi:10.5194/acp-8-4605-2008, 2008.

Atkinson, R.: Atmospheric chemistry of VOCs and NO_x, *Atmos. Environ.*, 34, 2063–2101, 2000.

Behnke, K., Ehling, B., Teuber, M., Bauerfeind, M., Louis, S., Hänsch, R., Polle, A., Bohlmann, J. and Schnitzler, J.-P.: Transgenic, non-isoprene emitting poplars don't like it hot, *Plant J.*, (51), 485–499, doi:10.1111/j.1365-313X.2007.03157.x, 2007.

485 Boeck, H. J. De and Verbeeck, H.: Drought-associated changes in climate and their relevance for ecosystem experiments and models, *Biogeosciences*, 8, 1121–1130, doi:10.5194/bg-8-1121-2011, 2011.

Brilli, F., Barta, C., Fortunati, A., Lerdau, M., Loreto, F. and Centritto, M.: Response of isoprene emission and carbon metabolism to drought in white poplar (*Populus alba*) saplings, *New Phytol.*, 175, 244–254, 2007.

490 Brilli, F., Tsonev, T., Mahmood, T., Velikova, V., Loreto, F. and Centritto, M.: Ultradian variation of isoprene emission , photosynthesis , mesophyll conductance , and optimum temperature sensitivity for isoprene emission in water-stressed *Eucalyptus citriodora* saplings, *Jounal Exp. Bot.*, 64(2), 519–528, doi:10.1093/jxb/ers353, 2013.

Brilli, F., Gioli, B., Fares, S., Terenzio, Z., Zona, D., Gielen, B., Loreto, F., Janssens, I. A. and Ceulemans, R.: Rapid leaf development drives the seasonal pattern of volatile organic compound (VOC) fluxes in a coppiced bioenergy poplar plantation, *Plant Cell Environ.*, 39, 539–555, doi:10.1111/pce.12638, 2016.

495 Carlton, A. G., Wiedinmyer, C. and Kroll, J. H.: A review of Secondary Organic Aerosol (SOA) formation from isoprene, *Atmos. Chem. Phys.*, 9(2), 4987–5005, doi:10.5194/acp-9-4987-2009, 2009.

Cierjacks, A., Kowarik, I., Joshi, J., Hempel, S., Ristow, M., von der Lippe, M. and Weber, E.: Biological Flora of the British Isles: *Robinia pseudoacacia*, *J. Ecol.*, 101, 1623–1640, doi:10.1111/1365-2745.12162, 2013.

500 Coumou, D. and Rahmstorf, S.: A decade of weather extremes, *Nat. Clim. Chang.*, 2, 491–496, doi:10.1038/nclimate1452, 2012.

Duarte, A. G., Katata, G., Hoshika, Y. and Hossain, M.: Immediate and potential long-term effects of consecutive heat waves on the photosynthetic performance and water balance in Douglas-fir, *J. Plant Physiol.*, 205, 57–66, doi:10.1016/j.jplph.2016.08.012, 2016.

505 Fortunati, A., Barta, C., Brilli, F., Centritto, M., Zimmer, I., Schnitzler, J.-P. and Loreto, F.: Isoprene emission is not temperature-dependent during and after severe drought-stress: a physiological and biochemical analysis, *Plant J.*, 55, 687–697, doi:10.1111/j.1365-313X.2008.03538.x, 2008.

Funk, J. L., Jones, C. G., Gray, D. W., Throop, H. L., Hyatt, L. A. and Lerdau, M. T.: Variation in isoprene emission from *Quercus rubra*: Sources, causes, and consequences for estimating fluxes, *J. Geophys. Res.*, 110(D4), D04301, doi:10.1029/2004JD005229, 2005.

510 Grote, R. and Niinemets, U.: Modeling volatile isoprenoid emissions -- a story with split ends., *Plant Biol.*, 10(1), 8–28, doi:10.1055/s-2007-964975, 2008.

Guenther, A.: Biological and Chemical Diversity of Biogenic Volatile Organic Emissions into the Atmosphere, *ISRN Atmos. Sci.*, 2013, Arti, 27pp, doi:10.1155/2013/786290, 2013.

515 Guenther, A. B., Monson, R. M. and Fall, R.: Isoprene and Monoterpene Emission Rate Variability: Observations With Eucalyptus and Emission Rate Algorithm Development, *J. Geophys. Res.*, 96(D6), 10799–10808, 1991.



520 Guenther, A. B., Zimmerman, P. R., Harley, P. C., Monson, R. K. and Fall, R.: Isoprene and Monoterpene Emission Rate Variability: Model Evaluations and Sensitivity Analyses, *J. Geophys. Res.*, 98(D7), 12609–12617, 1993.

525 Guenther, A., Karl, T., Harley, P., Wiedinmyer, C., Palmer, P. I. and Geron, C.: Estimates of global terrestrial isoprene emissions using MEGAN (Model of Emissions of Gases and Aerosols from Nature), *Atmos. Chem. Phys.*, 6, 3181–3210, doi:10.5194/acpd-6-107-2006, 2006.

530 Guenther, A. B., Jiang, X., Heald, C. L., Sakulyanontvittaya, T., Duhl, T., Emmons, L. K. and Wang, X.: The Model of Emissions of Gases and Aerosols from Nature version 2.1 (MEGAN2.1): an extended and updated framework for modeling biogenic emissions, *Geosci. Model Dev.*, 5(6), 1471–1492, doi:10.5194/gmd-5-1471-2012, 2012.

535 Hansel, A., Jordan, A., Holzinger, R., Prazeller, P., Vogel, W. and Lindinger, W.: Proton transfer reaction mass spectrometry: on-line trace gas analysis at the ppb level, *Int. J. Mass Spectrom.*, 149/150, 609–619, 1995.

540 Harrison, S. P., Morfopoulos, C., Dani, K. G. S., Prentice, I. C., Arneth, A., Atwell, B. J., Barkley, M. P., Leishman, M. R., Loreto, F., Medlyn, B. E., Niinemets, Ü., Possell, M., Penuelas, J. and Wright, I. J.: Volatile isoprenoid emissions from plastid to planet, *New Phytol.*, 197, 49–57, 2013.

545 Harvey, C. M., Li, Z., Tjellström, H., Blanchard, G. J. and Sharkey, T. D.: Concentration of isoprene in artificial and thylakoid membranes, *J. Bioenerg. Biomembr.*, 47, 419–429, doi:10.1007/s10863-015-9625-9, 2015.

550 Kaser, L., Karl, T., Guenther, A., Graus, M., Schnitzhofer, R., Turnipseed, A., Fischer, L., Harley, P., Madronich, M., Gochis, D., Keutsch, F. N. and Hansel, A.: Undisturbed and disturbed above canopy ponderosa pine emissions: PTR-TOF-MS measurements and MEGAN 2.1 model results, *Atmos. Chem. Phys.*, 13, 11935–11947, doi:10.5194/acp-13-11935-2013, 2013.

555 Kesselmeier, J. and Staudt, M.: Biogenic Volatile Organic Compounds (VOC): An Overview on Emission, Physiology and Ecology, *J. Atmos. Chem.*, 33, 23–88, 1999.

560 Kleinbauer, I., Dullinger, S., Peterseil, J. and Essl, F.: Climate change might drive the invasive tree Robinia pseudacacia into nature reserves and endangered habitats, *Biol. Conserv.*, 143, 382–390, doi:10.1016/j.biocon.2009.10.024, 2010.

565 Lathière, J., Hauglustaine, D. A., Friend, A. D., De Noblet-Ducoudré, N., Viovy, N. and Folberth, G. A.: Impact of climate variability and land use changes on global biogenic volatile organic compound emissions, *Atmos. Chem. Phys.*, 6, 2129–2146, 2006.

570 Lindinger, W., Hansel, A. and Jordan, A.: On-line monitoring of volatile organic compounds at pptv levels by means of Proton-Transfer-Reaction Mass Spectrometry (PTR-MS) Medical applications, food control and environmental research, *Int. J. Mass Spectrom.*, 173, 191–241, 1998.

575 Logan, B. A. and Monson, R. K.: Thermotolerance of Leaf Discs from Four Isoprene-Emitting Species Is Not Enhanced by Exposure to Exogenous Isoprene, *Plant Physiol.*, 120(3), 821–825, 1999.

580 Loreto, F. and Fineschi, S.: Reconciling functions and evolution of isoprene emission in higher plants, *New Phytol.*, 206, 578–582, doi:10.1111/nph.13242, 2015.

585 Loreto, F. and Schnitzler, J.-P.: Abiotic stresses and induced BVOCS, *Trends Plant Sci.*, 15(3), 154–66, doi:10.1016/j.tplants.2009.12.006, 2010.



560 Loreto, F., Barta, C., Brilli, F. and Nogues, I.: On the induction of volatile organic compound emissions by plants as consequence of wounding or fluctuations of light and temperature., *Plant Cell Environ.*, 29, 1820–1828, doi:10.1111/j.1365-3040.2006.01561.x, 2006.

Mantovani, D., Veste, M. and Freese, D.: Effects of Drought Frequency on Growth Performance and Transpiration of Young Black Locust (*Robinia pseudoacacia* L.), *Int. J. For. Res.*, 2014, doi:10.1155/2014/821891, 2014.

565 Monson, R. K., Jaeger, C. H., Adams III, W. W., Driggers, E. M., Silver, G. M. and Fall, R.: Relationships among Isoprene Emission Rate , Photosynthesis , and Isoprene Synthase Activity as Influenced by Temperature, *Plant Physiol.*, 98, 1175–1180, 1992.

Monson, R. K., Grote, R., Niinemets, Ü. and Schnitzler, J.-P.: Modeling the isoprene emission rate from leaves, *New Phytol.*, 195, 541–559, doi:10.1111/j.1469-8137.2012.04204.x, 2012.

570 Naik, V., Deliere, C. and Wuebbles, D. J.: Sensitivity of global biogenic isoprenoid emissions to climate variability and atmospheric CO₂, *J. Geophys. Res.*, 109(D06301), doi:10.1029/2003JD004236, 2004.

Ninemets, Ü.: Mild versus severe stress and BVOCs: thresholds, priming and consequences., *Trends Plant Sci.*, 15, 145–153, doi:10.1016/j.tplants.2009.11.008, 2010.

575 Niinemets, Ü., Tenhunen, J. D., Harley, P. C. and Steinbrecher, R.: A model of isoprene emission based on energetic requirements for isoprene synthesis and leaf photosynthetic properties for Liquidambar and Quercus, *Plant Cell Environ.*, 22, 1319–1335, 1999.

Ninemets, Ü., Loreto, F. and Reichstein, M.: Physiological and physicochemical controls on foliar volatile organic compound emissions., *Trends Plant Sci.*, 9(4), 180–6, doi:10.1016/j.tplants.2004.02.006, 2004.

580 Niinemets, Ü., Arneth, A., Kuhn, U., Monson, R. K., Penuelas, J. and Staudt, M.: The emission factor of volatile isoprenoids: stress, acclimation, and developmental responses, *Biogeosciences*, 7, 2203–2223, doi:10.5194/bg-7-2203-2010, 2010a.

Ninemets, Ü., Monson, R. K., Arneth, a., Ciccioli, P., Kesselmeier, J., Kuhn, U., Noe, S. M., Peñuelas, J. and Staudt, M.: The leaf-level emission factor of volatile isoprenoids: caveats, model algorithms, response shapes and scaling, *Biogeosciences*, 7(6), 1809–1832, doi:10.5194/bg-7-1809-2010, 2010b.

585 Niinemets, Ü., Kuhn, U., Harley, P. C., Staudt, M., Arneth, A., Cescatti, A., Ciccioli, P., Copolovici, L., Geron, C., Guenther, A., Kesselmeier, J., Lerdau, M. T., Monson, R. K. and Peñuelas, J.: Estimations of isoprenoid emission capacity from enclosure studies: measurements, data processing, quality and standardized measurement protocols, *Biogeosciences*, 8, 2209–2246, doi:10.5194/bg-8-2209-2011, 2011.

590 Pegeraro, E., Rey, A., Greenberg, J., Harley, P., Grace, J., Malhi, Y. and Guenther, A.: Effect of drought on isoprene emission rates from leaves of *Quercus virginiana* Mill., *Atmos. Environ.*, 38, 6149–6156, doi:10.1016/j.atmosenv.2004.07.028, 2004.

Potosnak, M. J., LeStourgeon, L., Pallardy, S. G., Hosman, K. P., Gu, L., Karl, T., Geron, C. and Guenther, A. B.: Observed and modeled ecosystem isoprene fluxes from an oakdominated temperate forest and the influence of drought stress, *Atmos. Environ.*, 84, 314–322, doi:10.1016/j.atmosenv.2013.11.055., 2013.

595 Rennenberg, H., Loreto, F., Polle, A., Brilli, F., Fares, S., Beniwal, R. S. and Gessler, A.: Physiological Responses of Forest Trees to Heat and Drought, *Plant Biol.*, (8), 556–571, doi:10.1055/s-2006-924084, 2006.

Ruehr, N. K., Gast, A., Weber, C., Daub, B. and Arneth, A.: Water availability as dominant control of heat stress responses in two contrasting tree species, *Tree Physiol.*, 36(2), 164–178, doi:10.1093/treephys/tpv102, 2016.

600 Schnitzler, J.-P., Graus, M., Heizmann, U., Kreuzwieser, J., Rennenberg, H., Wisthaler, A. and Hansel, A.: Contribution of Different Carbon Sources to Isoprene Biosynthesis in Poplar Leaves, *Plant Physiol.*, 135, 152–160, doi:10.1104/pp.103.037374.152, 2004.



Sharkey, T. D. and Loreto, F.: Water stress, temperature, and light effects on the capacity for isoprene emission and photosynthesis of kudzu leaves, *Oecologia*, 95(3), 328–333, doi:10.1007/BF00320984, 1993.

605 Sharkey, T. D. and Yeh, S.: Isoprene Emission From Plants., *Annu. Rev. Plant Phys.*, 52, 407–436, doi:10.1146/annurev.arplant.52.1.407, 2001.

Sharkey, T. D., Wiberley, A. E. and Donohue, A. R.: Isoprene emission from plants: why and how., *Ann. Bot.*, 101, 5–18, doi:10.1093/aob/mcm240, 2008.

Singsaas, E. L. and Sharkey, T. D.: The effects of high temperature on isoprene synthesis in oak leaves, *Plant Cell Environ.*, (23), 751–757, 2000.

610 Siwko, M. E., Marrink, S. J., de Vries, A. H., Kozubek, A., Schoot Uiterkamp, A. J. M. and Mark, A. E.: Does isoprene protect plant membranes from thermal shock? A molecular dynamics study., *Biochim. Biophys. Acta*, 1768(2), 198–206, doi:10.1016/j.bbapm.2006.09.023, 2007.

Staudt, M. and Peñuelas, J.: BVOCs and global change, *Trends Plant Sci.*, 15(3), 133–144, doi:10.1016/j.tplants.2009.12.005, 2010.

615 Velikova, V. and Loreto, F.: On the relationship between isoprene emission and thermotolerance in *Phragmites australis* leaves exposed to high temperatures and during the recovery from a heat stress, *Plant, Cell Environ.*, 28(3), 318–327, doi:10.1111/j.1365-3040.2004.01314.x, 2005.

620 Velikova, V., Várkonyi, Z., Szabó, M., Maslenkova, L., Nogues, I., Kovács, L., Peeva, V., Busheva, M., Garab, G., Sharkey, T. D. and Loreto, F.: Increased Thermostability of Thylakoid Membranes in Isoprene-Emitting Leaves Probed with Three Biophysical Techniques, *Plant Physiol.*, 157(2), 905–916, doi:10.1104/pp.111.182519, 2011.

Velikova, V., Sharkey, T. D. and Loreto, F.: Stabilization of thylakoid membranes in isoprene-emitting plants reduces formation of reactive oxygen species, *Plant Signal. Behav.*, 7(1), 139–141, doi:10.4161/psb.7.1.18521, 2012.

625 Velikova, V., Brunetti, C., Tattini, M., Doneva, D., Ahrar, M., Tsonev, T., Stefanova, M., Ganeva T., Gori, A., Ferrini, F., Varotto, C. and Loreto, F.: Physiological significance of isoprenoids and phenylpropanoids in drought response of Arundoideae species with contrasting habitats and metabolism, *Plant Cell Environ.*, 39, 2185–2197, doi: 10.1111/pce.12785, 2016.

630 Vickers, C. E., Gershenson, J., Lerdau, M. T. and Loreto, F.: A unified mechanism of action for volatile isoprenoids in plant abiotic stress., *Nat. Chem. Biol.*, 5(5), 283–291, doi:10.1038/nchembio.158, 2009.



635 **Table 1:** Results of a linear mixed-effects model evaluating isoprene emissions and photosynthesis (photosynthetic active radiation $> 50 \mu\text{mol m}^{-2}\text{s}^{-1}$) under different treatments and for different time-periods during the experiment (pre-treatment, heat period 1, recovery1, heat period 2 and recovery 2). The model tests for interactions between treatment and time-period relative to control conditions (ns means not significant, *** corresponds to a p-value < 0.005 and * corresponds to a p-value between 0.05 and 0.15).

Isoprene				
	value	SE	t-statistics	significance
Pre-treatment: Control (Intercept)	0.8	1.3	0.6	ns
Pre-treatment: Heat	0.1	1.2	0.1	ns
Pre-treatment: Heat-drought	1.4	1.2	1.1	ns
Stress period 1	1.2	1.3	0.9	ns
Recovery 1	0.2	1.5	0.1	ns
Stress period 2	0.2	1.3	0.1	ns
Recovery 2	-0.4	1.5	-0.3	ns
Heat x stress period 1	4.4	1.1	3.8	***
Heat-drought x stress period 1	3.4	1.2	3.0	***
Heat x Recovery 1	0.2	1.2	0.1	ns
Heat-drought x recovery 1	-0.6	1.2	-0.5	ns
Heat x stress period 2	1.8	1.1	1.6	*
Heat-drought x stress period 2	4.0	1.1	3.6	***
Heat x recovery 2	-0.2	1.2	-0.1	ns
Heat & drought x recovery 2	-1.3	1.2	-1.1	ns
Photosynthesis				
	value	SE	t-statistics	significance
Pre-treatment: Control (Intercept)	4.6	0.8	5.9	***
Pre-treatment: Heat	0.0	0.8	0.0	ns
Pre-treatment: Heat-drought	-0.8	0.8	-1.1	ns
Stress period 1	0.0	1.2	0.0	ns
Recovery 1	0.8	1.6	0.5	ns
Stress period 2	1.0	1.2	0.8	ns
Recovery 2	1.0	1.9	0.5	ns
Heat x stress period 1	-1.9	0.7	-2.8	***
Heat-drought x stress period 1	-1.9	0.7	-2.8	***
Heat x Recovery 1	-1.1	0.9	-1.2	ns
Heat-drought x recovery 1	0.4	0.9	0.4	ns
Heat x stress period 2	-2.6	0.6	4.1	***
Heat-drought x stress period 2	-1.9	0.6	3.0	***
Heat x recovery 2	-1.7	1.1	-1.5	*
Heat & drought x recovery 2	-0.4	1.0	-0.4	ns



645

Table 2: Ratio between assimilated carbon and carbon emitted as isoprene (C_{iso}/C_A) averaged for different temperature ranges and treatments during the stress periods including the corresponding standard deviation (calculated using data points with $PAR > 50 \mu\text{mol m}^{-2}\text{s}^{-1}$ only). The number of values (n) included in the calculation of the class averages is given to the right of each C_{iso}/C_A column. C_{iso}/C_A values were only significantly different ($p < 0.05$, u-test) between the control and heat treatment in the temperature range 28°C-32°C.

Treatment	Control		Heat		Heat-drought	
	Temperature range (°C)	C_{iso} / C_A (%)	n	C_{iso} / C_A (%)	n	C_{iso} / C_A (%)
15-20	0.1±0.03	2	---	0	---	0
20-24	0.3±0.1	16	---	0	---	0
24-28	0.5±0.2	15	0.6*	1	0.8±0.3	2
28-32	1.6±0.7	12	0.8±0.3	15	1.2±0.7	29
32-35	---	0	1.7±0.7	29	3.0±2.5	32
35-40	6.5*	1	5.3±6.0	38	10.0±16.4	49
40-45	---	0	10.9±6.4	17	20.2±16.5	25
>45	---	0	12.5*	1	12.0±5.4	5

* single value

650

655

Table 3: Parameters $E_S * C_{L1}$ (E_S being the isoprene emission factor at standardized conditions and C_{L1} a dimensionless scaling parameter) and α including their corresponding standard errors and the t-statistic for the optimized light response curve of the control heat and heat-drought trees at a standard temperature of 30°C. The parameters E_S [$\mu\text{mol m}^{-2}\text{s}^{-1}$], C_{T1} [J mol^{-1}], C_{T2} [J mol^{-1}] and the temperature optimum of isoprene emissions T_m [K] (with corresponding standard errors SE and t-statistic) derived for the temperature response curve at a standard photosynthetic active radiation of $500 \mu\text{mol m}^{-2} \text{s}^{-1}$ are shown in an analog manner. Values with a p-value ≤ 0.05 are highlighted bold letters.

		Light response curve		Temperature response curve			
		$E_S * C_{L1}$	α	EF	C_{T1}	C_{T2}	T_m
Control	value	16.2	0.0070	16.0	$1.42 * 10^5$	$5.08 * 10^5$	311.80
	SE	1.4	0.002	0.2	$0.05 * 10^5$	$0.83 * 10^5$	n.v.
	t-statistic	11.5	4.1	74.8	29.2	6.1	n.v.
Heat	value	9.5	0.0043	8.7	$1.38 * 10^5$	$2.83 * 10^5$	315.5
	SE	0.4	0.0004	0.5	$0.13 * 10^5$	$0.25 * 10^5$	1.0
	t-statistic	22.5	11.2	17.7	10.7	11.5	318.8
Heat-drought	value	12.8	0.0037	12.1	$1.01 * 10^5$	$2.80 * 10^5$	314.3
	SE	0.7	0.0004	1.2	$0.25 * 10^5$	$0.46 * 10^5$	2.0
	t-statistic	17.7	8.4	10.2	4.0	6.1	155.2

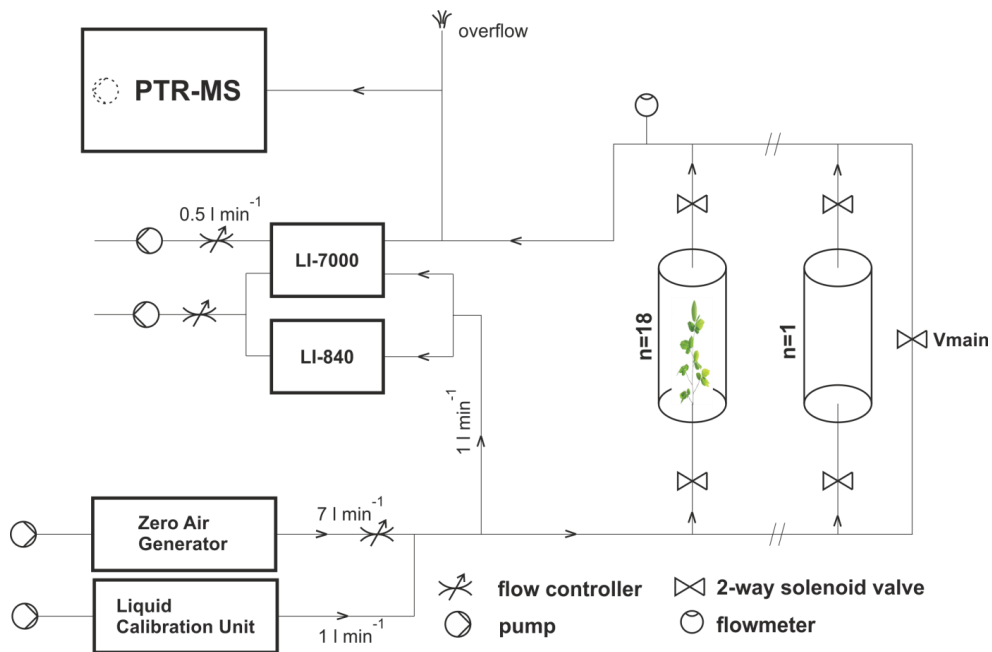


Figure 1: Schematic of the automated leaf chamber measurement set-up. Note that for simplification the setup is shown for two chambers, but was extended to 9 branch chambers and one empty chamber measured in sequence.
660 The direction of the air flow is indicated by the small arrows.

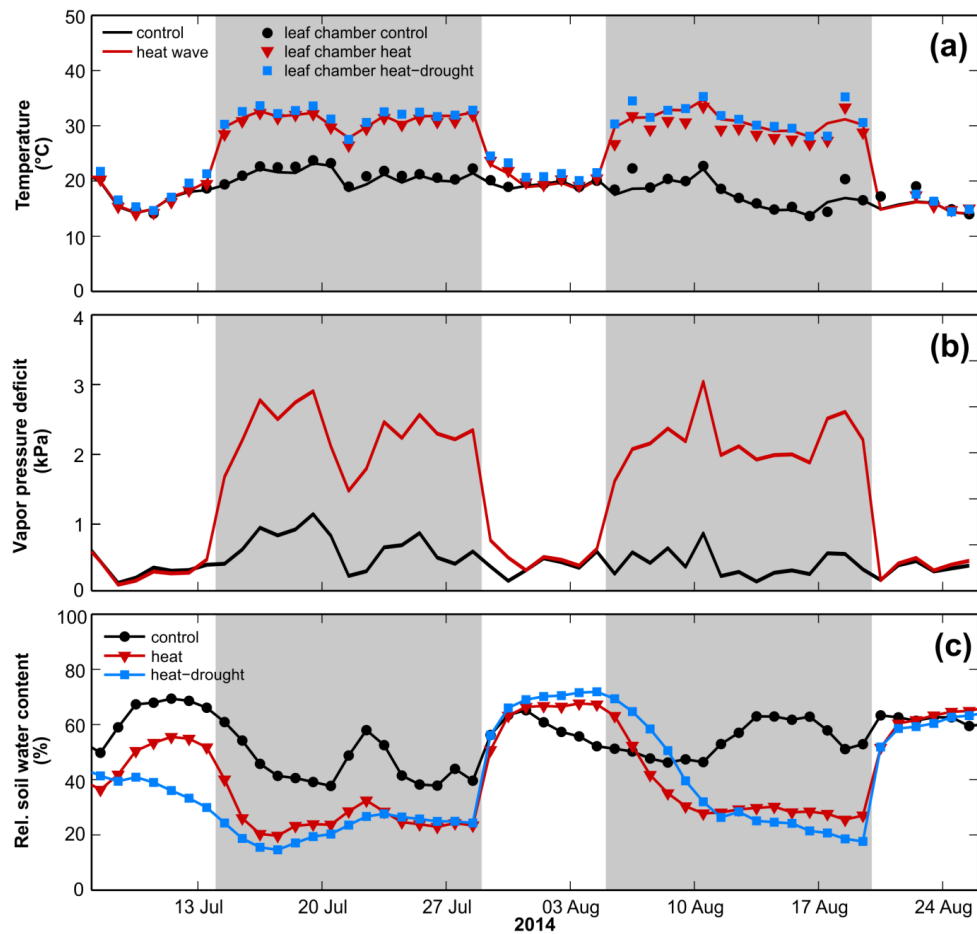


Figure 2: Daily average temperatures (panel a) in the control (black line) and stress (red line) compartment of the greenhouse and in the plant chambers of the control (black circles), heat (red triangles) and heat-drought (blue squares) treatments. Daily average vapor pressure deficit (panel b) in the control (black line) and heat (red line) compartment of the greenhouse and relative soil water content (panel c) averaged for each treatment (control – black line and symbol, heat – red line and symbol, heat-drought – blue line and symbol) and measurement day. Heat waves are represented by the grey colored areas.

665

670

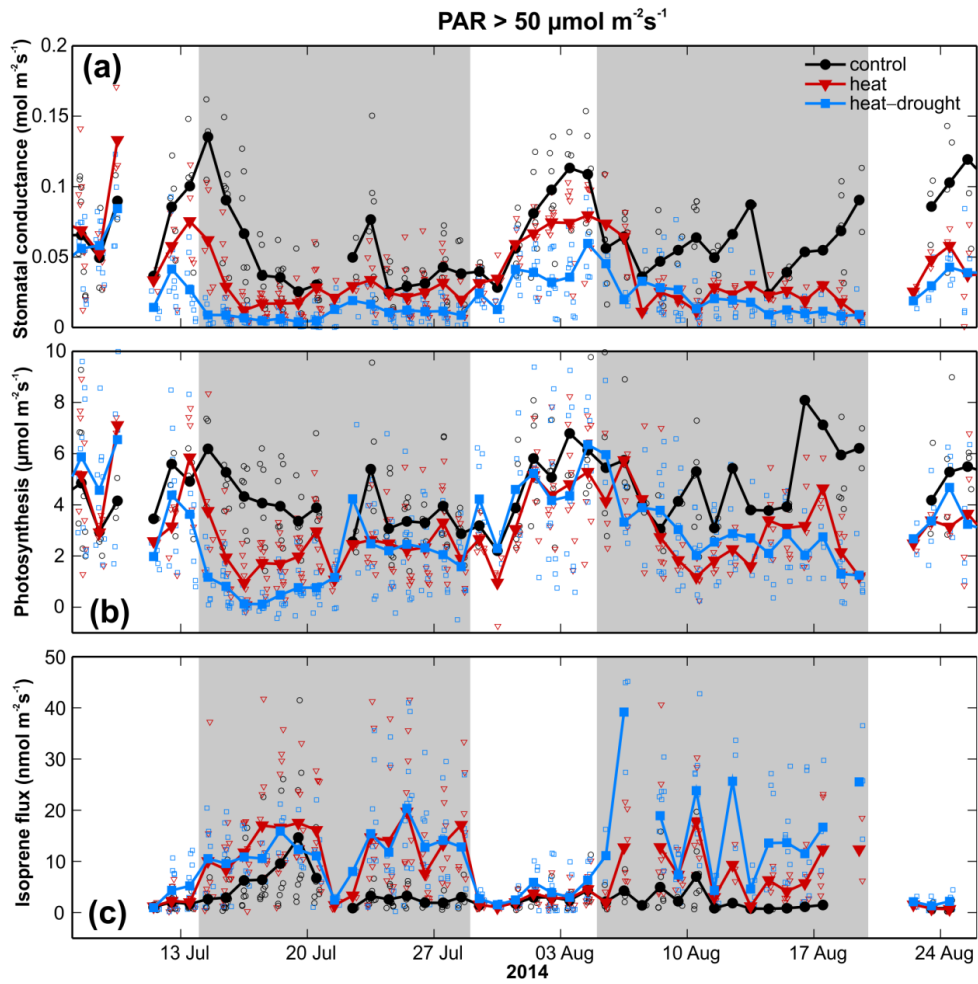
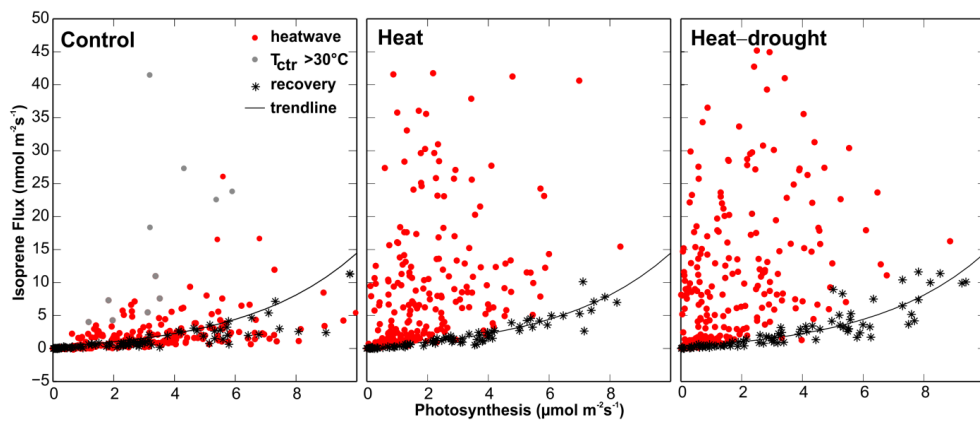


Figure 3: Daytime (PAR $> 50 \mu\text{mol m}^{-2}\text{s}^{-1}$) values for stomatal conductance (panel a) photosynthesis (panel b) and isoprene emission (panel c) of black locust trees for the control (black circles), heat (red triangles) and combined heat-drought treatment (blue squares). Filled symbols and lines are daytime averages on average consisting of seven single chamber measurements. Heat waves are represented by the grey colored areas.

675



680 **Figure 4:** Relationship of isoprene emission with photosynthesis ($A > 0 \mu\text{mol m}^{-2}\text{s}^{-1}$) in black locust trees during the two heat waves (red and grey circles; grey circles distinguish points when the temperature in the control chambers exceeded 30°C) and recovery periods (black asterisks) shown in separate panels for the control, heat and heat-drought treatment. Solid lines represent an exponential curve of the form $y=\exp^{(a \cdot x)}-\beta$ which was derived from a non-linear fit to the measurements of heat-drought stressed trees during recovery to describe the dependency between photosynthesis and isoprene emission exemplarily.

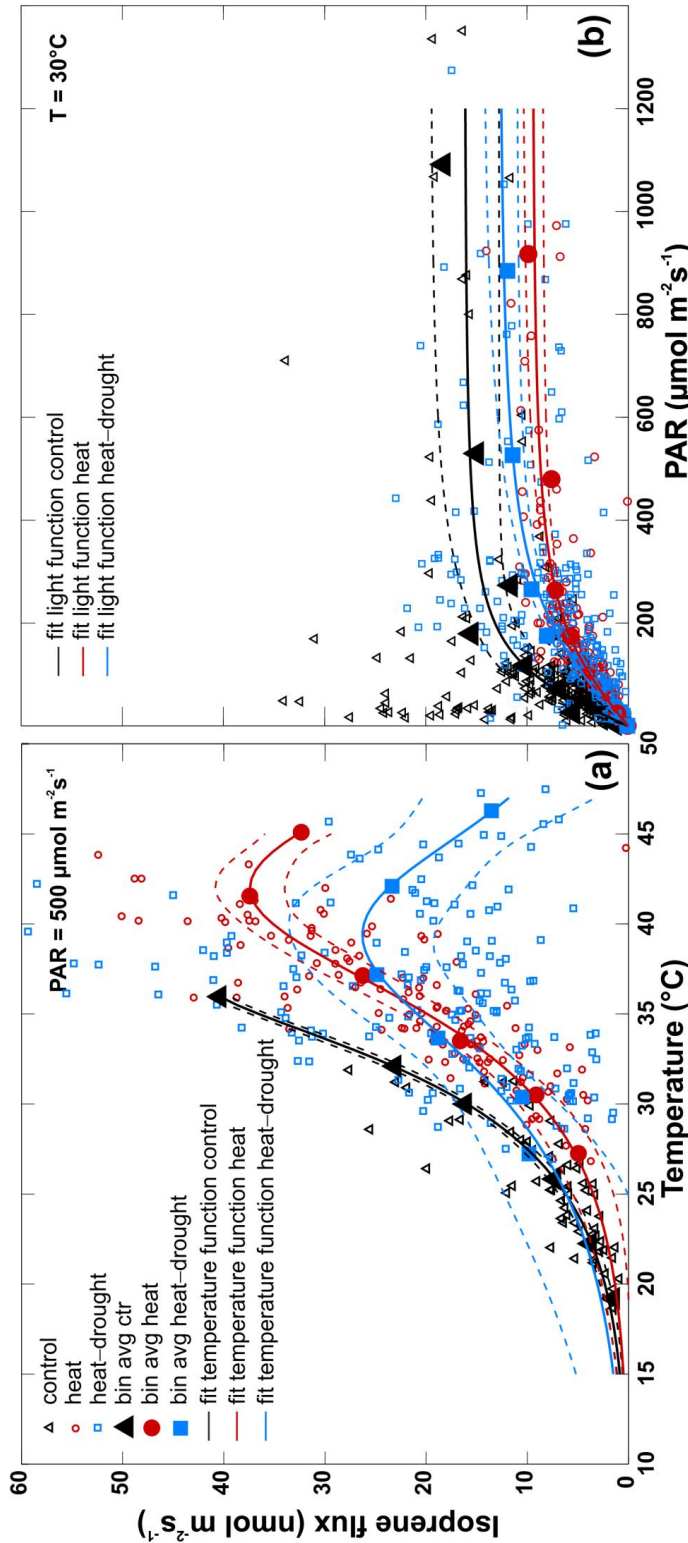


Figure 5: Dependency of isoprene emissions on temperature (panel a; daytime isoprene emissions, $\text{PAR} > 50 \mu\text{mol m}^{-2} \text{s}^{-1}$, normalized to $\text{PAR} = 500 \mu\text{mol m}^{-2} \text{s}^{-1}$) and light (panel b; normalized to $T = 30^{\circ}\text{C}$) in black locust trees during the heat waves. Filled symbols are bin averages for predefined temperature or light classes in the control (black), heat (red) and heat-drought treatment (blue). Single data points are depicted by open symbols. Solid lines are derived by non-linear regression of averaged isoprene emissions to temperature and light response functions (Eq. (7) and (8)). Dashed lines are the respective 95 % confidence intervals of the regression fits.